Nanometer Scale Observation of High Efficiency Thermally Assisted Current-Driven Domain Wall Depinning

D. Ravelosona,[1] D. Lacour,[1] J. A. Katine,[1] B. D. Terris,[1] and C. Chappert[2]

[1]*Hitachi Global Storage Technologies, San Jose Research Center, 650 Harry Road, San Jose, California, 95120 USA*
[2]*Institut d'Electronique Fondamentale, UMR CNRS 8622, Université Paris Sud, 91405 ORSAY Cedex, France*

(Received 8 February 2005; published 8 September 2005)

Nanometer scale observation of the depinning of a narrow domain wall (DW) under a spin current is reported. We studied ~12 nm wide 1D Bloch DWs created in thin films exhibiting perpendicular magnetic anisotropy. Magnetotransport measurements reveal thermally assisted current-driven DW motion between pinning sites separated by as little as 20 nm. The efficiency of current-driven DW motion assisted by thermal fluctuations is measured to be orders of magnitude higher than has been found for in-plane magnetized films, allowing us to control DW motion on a nanometer scale at low current densities.

DOI: 10.1103/PhysRevLett.95.117203 PACS numbers: 75.60.Ch, 72.25.Ba, 75.75.+a

Much recent experimental [1–10] and theoretical [11–14] work has focused on current-driven motion of domain walls (DW) in magnetic wires, building on Berger's pioneering work [15,16]. Understanding the mechanisms behind current-induced domain wall motion remains a challenging problem. All previous measurements of current-driven DW motion have used in-plane magnetized wires having a 3D Néel-type DW configuration. Since the DW width is large (~100 nm), these experiments are expected to have investigated only the ''adiabatic'' limit [15] for which the DW is wide enough to allow the electron spin to follow the local magnetization direction, with transfer of spin momentum. Also, such a wide DW integrates local variations in the pinning potential, making it difficult to probe the depinning process on a nanometer scale, the length scale expected for intrinsic pinning sites. As a consequence, the critical current density J_c has been inferred from micron scale observation [1–10] of steady DW motion (velocities ~m/s), giving rise to J_c values above the real threshold depinning current density, J_{td}. Also, a remaining question is whether currents $J < J_{td}$ can induce DW motion in the presence of thermal excitations.

Using a very narrow 1D Bloch DW created in thin films with perpendicular magnetic anisotropy (PMA), we are able to explore, for the first time, the nonadiabatic limit as well as the role of thermal excitations in current-driven domain wall motion. In spite of a strong pinning potential, we find an unexpectedly low value for the critical current density required to excite domain wall motion.

Our films are $F1/\mathrm{Cu}/F2$ spin valves with $F1$ and $F2$ both exhibiting PMA. $F1/\mathrm{Cu}/F2$ consist of a $[\mathrm{Co}(0.5)/\mathrm{Pt}(1)]_4/\mathrm{Co}(0.5)/\mathrm{Cu}(6)/\mathrm{Co}(0.5)/\mathrm{Pt}(3)$ multilayer grown on a high quality $\mathrm{Si}/\mathrm{Si_3N_4}/\mathrm{Pt}(1)/\mathrm{Au}(20)/\mathrm{Pt}(5)$ (thicknesses given in nm) buffer layer [17]. $F1$ acts as the reference layer due to the higher PMA of the [Co/Pt] multilayers ($\sim 2 \times 10^7$ erg/cm^3), while the free layer $F2$ having a single Co/Pt interface exhibits a lower PMA ($\sim 6 \times 10^6$ erg/cm^3). As shown in Fig. 1(a), because of their different PMAs the free and reference layers reverse at distinct magnetic fields. In addition to producing narrower DWs than in-plane spin valves, this perpendicular configuration has the advantage that the in-plane Oersted field created in the $F1$-$F2$ layers by the current in the spin valve cannot move the DW. Furthermore, DWs in the free layer can be treated as nearly perfect 1D Bloch walls with a typical width of $\Delta = 12$ nm [18,19]. These can be consid-

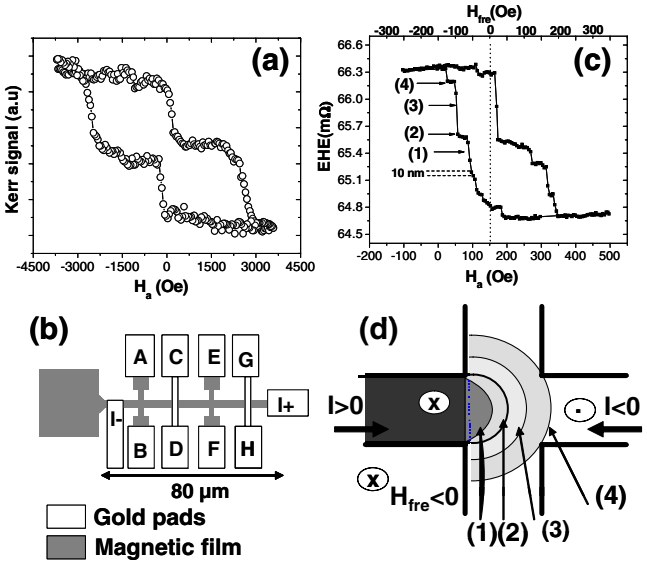

FIG. 1 (color online). (a) Polar Kerr hysteresis loop of our $F1/\mathrm{Cu}/F2$ spin valves with PMA measured in a continuous film. (b) Schematic diagram of a top view of the device. (c) EHE minor hysteresis loop corresponding to the reversal of the free layer in a 200×200 nm^2 Hall cross. A small EHE jump corresponding to DW motion over 10 nm is indicated. The EHE values (1) to (4) refer to the positions indicated in Fig. 1(d). (d) Bubblelike behavior of an ideal 1D Bloch DW in a magnetic Hall cross. This process has been demonstrated previously by Kerr microscopy [18,20]. The electron flow direction is indicated by the horizontal arrows.

ered as model systems compared to complicated 3D Néel walls.

Following the multilayer deposition, 100 μm long, 200 nm wide wires were fabricated by means of electron beam lithography and ion milling. Our sample geometry is depicted in Fig. 1(b). We have used the extraordinary Hall effect (EHE) which is proportional to the perpendicular magnetization to detect DW motion inside one of the magnetic Hall cross (contacts *E*-*F*) [18–20]. A large reservoir at the end of the magnetic wire is used to inject a single DW into the wire. The giant magnetoresistance effect (GMR) was used to yield information about DW motion in the wires (contacts *C*-*G*). The GMR and EHE have been measured using a high sensitivity ac ($\sim$10 μA) Wheatstone bridge with the magnetic field H_a applied perpendicular to the film. The dc current has been injected by using a bias *T*. Figure 1(c) shows a typical EHE minor hysteresis loop corresponding to the reversal of the *F*2 free layer by propagation of a single DW through the 200×200 nm^2 Hall cross (contacts *E*-*F*). The 3% variation of the EHE resistance allows us to detect the DW motion on a scale as small as 10 nm, such as the jump indicated in Fig. 1(c). The loop is offset in field by $H_d = -140$ Oe which is consistent with the calculation of the dipolar stray field from the reference layer whose magnetization is pointing down here [21]. The Cu layer is thick enough (6 nm) to reduce the orange peel effect and the RKKY coupling. The net perpendicular field in the free layer is thus $H_{\mathrm{fre}} = H_a + H_d$.

In Fig. 1(c) the wide plateaus present near 50% EHE amplitude on both branches of the minor loop is a clear signature of DW pinning. It has been already demonstrated [18–20] that this pinning results from a soap-bubble-like bending of the DW inside the Hall cross to minimize its energy as illustrated in Fig. 1(d). The maximum of pinning is obtained when the DW reaches the cross center [semicircle at position (2) corresponding to the plateaus in Fig. 1(c)]. With a perfect 1D Bloch DW this maximum corresponds to a topologically induced pinning field $H_{\mathrm{top}} = (\sigma/w_{M_S})$, w being the wire width and σ the wall energy. Using typical values for our system, we find $H_{\mathrm{top}} = 300$ Oe. In addition, homogeneously distributed nanometer-scale structural defects affect DW motion, so the total pinning field corresponding to position (2) for the bent DW is $\mathrm{H}_p = H_{\mathrm{pi}} + H_{\mathrm{top}}$, where H_{pi} is the intrinsic pinning field due to the structural pinning potential of the virgin films. Time resolved EHE measurements can be used to determine the pinning strength at this position (2) [20]. For that, the time of depinning $\tau(H_{\mathrm{fre}}, I = 0)$ at position (2) was measured as a function of a constant field H_{fre} at zero dc current. Our results can be fit [17] to a classical thermally activated depinning behavior [20,22] described by:

$$\tau(H_{\mathrm{fre}}, I = 0) = \tau_0 \exp[2M_S V(H_P - H_{\mathrm{fre}})/k_B T], \quad (1)$$

where V is an activation volume, M_S the saturation magnetization, τ_0 an intrinsic depinning time, and $k_B T$ the thermal energy. This relation emphasizes that the DW can be depinned at fields H_{fre} much lower than H_p by thermal activation. Assuming a typical value $\tau_0 \sim 1$ ns [22], we find $H_p = 400$ Oe which leads to an intrinsic pinning field $H_{\mathrm{pi}} = H_p - H_{\mathrm{top}} = 100$ Oe consistent with the value found in our continuous films [17]. Note that H_p also integrates any local variation in H_d along the DW [21].

To study the effect of a dc current on pinning, the sample is first prepared with a DW frozen at a position (2), and then the current I is increased by steps of 0.1 mA in time intervals of $\Delta t = 1$ s. The motion of the DW in the Hall cross is determined from the value of the EHE resistance [18]. Here, we focus on the negative branch of the loop (i.e., $H_p = -400$ Oe) where at $I = 0$ only the range $-65 < H_{\mathrm{fre}} < 0$ leads to a relatively stable (>1 hour) pin-

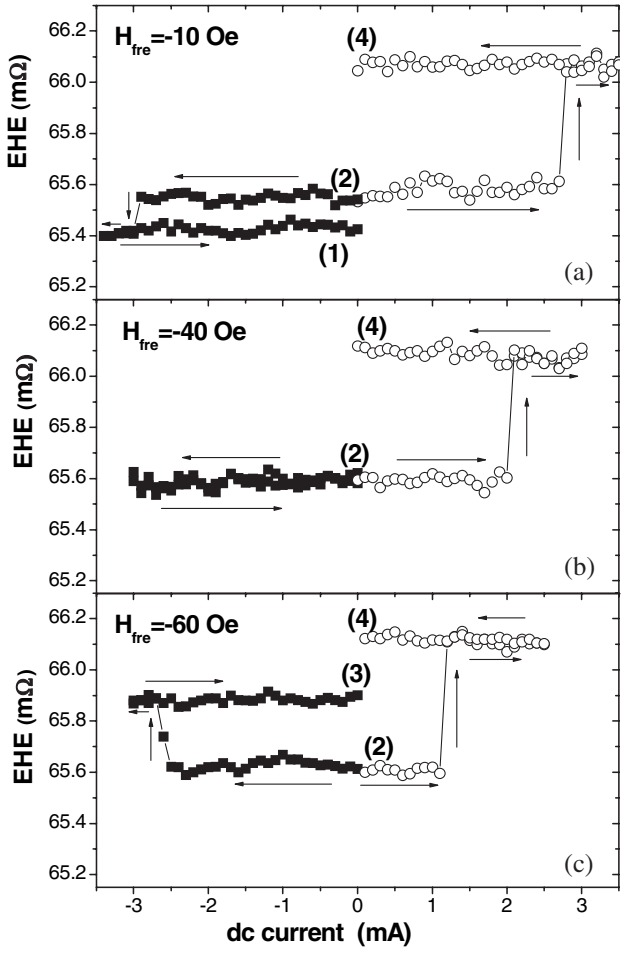

FIG. 2. EHE as a function of the applied dc current for fields (a) $H_{\mathrm{fre}} = -10$ Oe, (b) $H_{\mathrm{fre}} = -40$ Oe, and (c) $H_{\mathrm{fre}} = -60$ Oe. Measurements have been done by increasing the current from $I = 0$ to $I = \pm 3$ mA and then reducing it to $I = 0$, with a DW initially pinned at position (2). The negative (closed symbols) and positive (open symbols) current measurements have been realized independently. The states (1) to (4) refer to the positions in Fig. 1(d). The small Joule heating contribution has been subtracted.

ning at position (2). Figure 2 shows the EHE resistance as a function of the dc current for net fields $H_{\rm fre} = -10$, -40, and -60 Oe in the free layer. For a positive current above a critical value $I_{c+}(H_{\rm fre})$, the DW abruptly moves from position (2) to position (4) (exit of the Hall cross), which corresponds to a distance of $\sim$90 nm. When the field is increased, I_{c^+} is reduced and the dependence of I_{c^+} on $H_{\rm fre} \leq 0$ is illustrated in Fig. 3. We find a monotonic variation given by $I_{c+}(H_{\rm fre}) = I_{c+}(0)[1 - H_{\rm fre}/H_0]$ where $I_{c^+}(0) = 3.6$ mA and $H_0 = -95$ Oe.

In our system, given the complicated structure of our $F1/{\rm Cu}/F2$ multilayer and the fact that the current flows primarily in the Au layer [17], it is a difficult task to calculate the current density in the 0.5 nm thick Co layer. However, if we assume independent conduction between the Au and the spin valve stack, neglecting the possible shunting by the Cu, we estimate a low critical current density at zero field of $J_c(0) \sim 1 \times 10^7$ A/cm^2.

As shown in Fig. 2(a), for a negative current exceeding $I_{c-}(-10\ {\rm Oe}) = -2.9$ mA, the DW moves in the opposite direction, from position (2) to (1), over a smaller distance of $\sim$20 nm, against the pressure exerted by the net field. This behavior has been observed for net fields -20 Oe $< H_{\rm fre} < 0$ Oe. By increasing the field up to $H_{\rm fre} = -40$ Oe [Fig. 2(b)], a negative current up to a limit of -3 mA has no effect, whereas at $H_{\rm fre} = -60$ Oe [Fig. 2(c)], the DW once depinned by a negative current moves over a distance of $\sim$45 nm [position (3)] in the direction of the field pressure, as one might expect due to the larger net field opposing negative current-driven motion.

In order to determine whether thermal fluctuations are likely to play an important role in current-driven DW depinning, we have investigated the current dependence of the depinning time $\tau(I, H_{\rm fre})$ at position (2) (see inset to Fig. 4 for details). At the highest current densities we applied, the temperature rise due to current-induced Joule heating is less than 20 K as determined from the variation of the EHE resistance. By heating the sample at $I = 0$, we have checked that this temperature rise cannot by itself depin the DW. As illustrated in Fig. 4, the depinning time $\tau(H_{\rm fre}, I)$ decreases exponentially with increasing current for $H_{\rm fre} = -40$ Oe. Such a behavior is consistent with a thermally activated process of the form:

$$\tau(H_{\rm fre}, I) = \tau_0 \exp[A(I_{\rm td}(H_{\rm fre}) - I)/k_B T], \qquad (2)$$

where A is a constant, τ_0 is the same depinning time as in Eq. (1), I the applied current, and $I_{\rm td}(H_{\rm fre})$ the critical current in absence of thermal fluctuations. The field dependence of $I_{\rm td}(H_{\rm fre})$ can be deduced from comparing Eq. (1) with Eq. (2) for $I = 0$. We find $I_{\rm td}(H_{\rm fre}) = I_{\rm td}(0) \times (1 - H_{\rm fre}/H_p)$ where $I_{\rm td}(0) = H_p(2M_S V/A)$. The fit to the experimental data related to Eqs. (1) and (2) gives the slopes A/kT and $2M_S V/kT$, which leads to $(A/2M_S V) \sim 50$ Oe/mA and $I_{\rm td}(H_{\rm fre} = 0) = 8$ mA using $H_p = 400$ Oe. Therefore, $J_{\rm td}(0)/J_c(0) \sim 2.3$, which emphasizes the important role played by thermal fluctuations in current-driven DW depinning processes. Substituting $I_{\rm td}(H_{\rm fre}) = I_{\rm td}(0)(1 - H_{\rm fre}/H_p)$ into Eq. (2), we find that the energy barrier for current-induced DW depinning is $E(H_{\rm fre}, I) = 2M_S V[H_P + (A/2M_S V)I - H_{\rm fre}]$. So an important result is that the current I is equivalent to a huge effective perpendicular field $H_I = (A/2M_S V)I$ opposing to H_p.

Because of the ultrathin character of the free layer, the classical hydromagnetic domain drag force associated with the curvature of the current lines can be neglected [16]. Transfer of linear momentum can also be excluded since it is expected to be efficient only for a DW width of the order of the Fermi wavelength [11] or for current-induced DW resonance at high frequencies [9]. We believe a spin transfer mechanism [11–15] should be the main source of our observed current-driven DW motion. Since

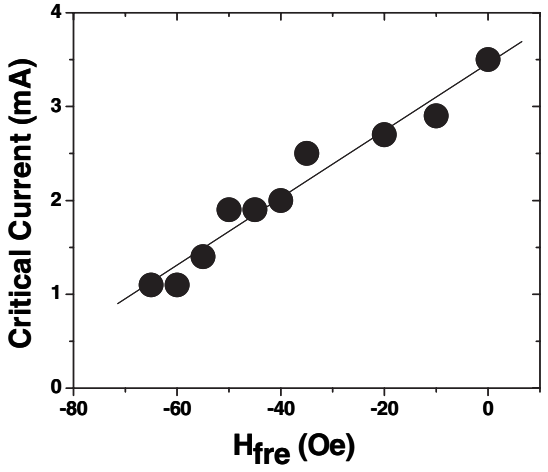

FIG. 3. Critical positive current as a function of $H_{\rm fre} \leq 0$ with a DW initially pinned at position (2) in Fig. 1(d).

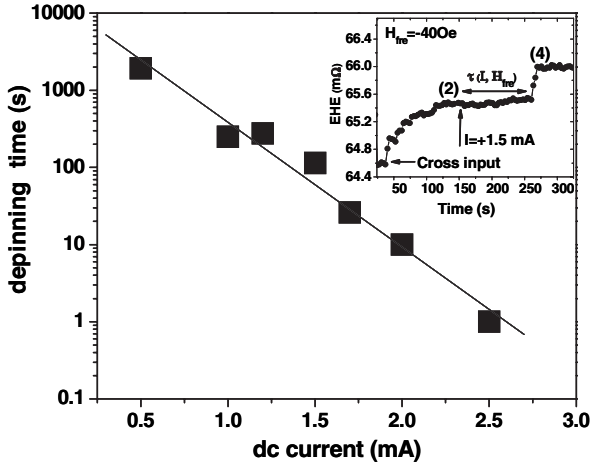

FIG. 4. Depinning time $\tau(I, H_{\rm fre})$ at position (2) as a function of dc current for $H_{\rm fre} = -40$ Oe. Inset: typical measurement of $\tau(I, H_{\rm fre})$ for a DW initially at the cross input. Under $H_{\rm fre} = -40$ Oe, the DW propagates by discrete jumps of about 10 nm until it remains pinned at position (2) [cf. Fig. 1(d)]. Then a dc current I is applied (in this case, $+1.5$ mA) and the depinning time, $\tau(I, H_{\rm fre})$, is measured.

the DW width in our sample is of the order the Larmor precession length [12], we would expect the spin transfer efficiency to be reduced as the electron spins are not fully reversed while crossing the narrow DW. Moreover, the pinning force in our PMA samples is ~tens times stronger than it is for standard in-plane magnetized samples. Despite these effects, we measure a critical current density $J_c(0) \sim 10^7$ A/cm^2 [$J_{td}(0) \sim 2 \times 10^7$ A/cm^2 without thermal fluctuations], similar to the lowest value found for in-plane magnetized metallic wires [3], and indicates in our case a much higher efficiency of the current-induced force on the DW. In order to quantify this efficiency, we calculate the force per unit current F applied to the DW as described in Ref. [6] which allows a direct comparison. This force is given by the effective field pressure originating from the current ($2M_S H_I$) per current density unit. We find a large force per current unit of $\sim 2 \times 10^{-7}$ NA^{-1}, i.e., ~500 times higher than the values found for in-plane magnetized samples [6,16].

In order to explain such a high efficiency, we want to emphasize a major point. In previous experiments, the critical current density has been determined from observation of 3D Néel walls motion on a micron scale and in the m/s velocity range [1–10,16], leading to critical current values above the real threshold depinning current J_{td}. Conversely, in our measurements the current does not drive the wall over a long distance, but rather depins a static 1D DW in presence of thermal fluctuations below J_{td} and displaces the wall between 2 metastable states. One striking feature is that these two regimes involve quite distinct dynamical magnetization processes. Recent theories have confirmed [11,14] that spin momentum transfer can drive for $J > J_{td}$ a steady motion of the DW by continuous precession of the DW magnetization. In this precessional regime, the complicated spin structure of a 3D-Néel wall can be transformed by a current, inducing a reduction of the spin transfer efficiency [23]. In addition, as for the viscous regime under a magnetic field [22], the spin momentum transfer might be strongly reduced by damping through, for example, excitations of spin waves as invoked in Ref. [7]. Conversely, in our simple 1D DW case, for current-induced forces below J_{td}, the DW motion proceeds by thermally activated jumps over energy barriers. In this quasistatic regime for which the pinning potential landscape plays the major role, the 1D DW structure is very rigid [19], and unlike a precessional motion regime, damping processes are negligible. As a consequence, the spin transfer efficiency is expected to be much higher. Note that the presence of a strong spin orbit interaction provided by the top Pt layer does not seem to alter the efficiency, in agreement with Ref. [10].

In conclusion, by using a very narrow DW, we have observed, on a nanometer scale, thermally assisted DW motion driven by a current with very high spin momentum transfer efficiency. Our demonstration of controllable DW motion on a scale of ~20 nm might be potentially important for ultrahigh density spintronic devices.

Fruitful discussions with J. Sun, M. Viret, and E. Fullerton are gratefully acknowledged.

[1] L. Gan, S. H. Chung, K. H. Ashensbach, M. Dreyer, and R. D. Gomez, IEEE Trans. Magn. **36**, 3047 (2000).
[2] H. Koo, C. Krafft, and R. D. Gomez, Appl. Phys. Lett. **81**, 862 (2002).
[3] J. Grollier *et al.*, Appl. Phys. Lett. **83**, 509 (2003).
[4] M. Klaui *et al.*, Appl. Phys. Lett. **83**, 105 (2003).
[5] M. Tsoi, R. E. Fontana, and S. S. Parkin, Appl. Phys. Lett. **83**, 2617 (2003).
[6] N. Vernier *et al.*, Europhys. Lett. **65**, 526 (2004).
[7] A. Yamaguchi *et al.*, Phys. Rev. Lett. **92**, 077205 (2004).
[8] C. K. Lim *et al.*, Appl. Phys. Lett. **84**, 2820 (2004).
[9] E. Saitoh, H. Miyajima, T. Yamaoka, and G. Tatara, Nature (London) **432**, 203 (2004).
[10] M. Yamanouchi, D. Chiba, F. Matsukura, and H. Ohno, Nature (London) **428**, 539 (2004).
[11] G. Tatara and H. Kohno, Phys. Rev. Lett. **92**, 086601 (2004).
[12] X. Waintal and M. Viret, Europhys. Lett. **65**, 427 (2004).
[13] Z. Li and S. Zhang, Phys. Rev. Lett. **92**, 207203 (2004); S. Zhang and Z. Li, Phys. Rev. Lett. **93**, 127204 (2004).
[14] A. Thiaville, Y. Nakatani, J. Miltat, and Y. Susuki, Europhys. Lett. **69**, 990 (2005).
[15] L. Berger, J. Appl. Phys. **49**, 2156 (1978); **55**, 1954 (1984).
[16] P. P. Freitas and L. Berger, J. Appl. Phys. **57**, 1266 (1985); C. Hung and L. Berger, J. Appl. Phys. **63**, 4276 (1988).
[17] D. Ravelosona, D. Lacour, J. Katine, and B. Terris, IEEE Trans. Magn. (to be published).
[18] J. Wunderlich *et al.*, IEEE Trans. Magn. **37**, 2104 (2001).
[19] F. Cayssol *et al.*, Phys. Rev. Lett. **92**, 107202 (2004).
[20] D. Ravelosona *et al.*, J. Magn. Magn. Mater. **249**, 170 (2002).
[21] Calculations indicate that the interstack (from the reference layer $F1$) and intrastack (within $F2$) stray fields are constant (-150 and 0 Oe, respectively) all along the DW in $F2$ except very close (~20 nm) to the cross corners.
[22] J. Ferre, *Spin Dynamics in Confined Magnetic Structures I* (Springer, New York, 2002), Vol. 83, p. 127.
[23] M. Klaui *et al.*, Phys. Rev. Lett. **95**, 026601 (2005).